Journal of Applied Polymer Science

Films made from poly(vinyl alcohol-*co*-ethylene) and soluble biopolymers isolated from postharvest tomato plant

Flavia Franzoso,[1] Diego Antonioli,[2] Enzo Montoneri,[3] Paola Persico,[4] Silvia Tabasso,[5] Michele Laus,[2] Raniero Mendichi,[4] Michele Negre,[6] Carlos Vaca-Garcia[7]

[1]Dipartimento di Chimica, Università di Torino, 10125 Torino, Italy
[2]Dipartimento di Scienze e Innovazione Tecnologica (DISIT), Università degli Studi del Piemonte Orientale "A. Avogadro," INSTM, UdR Alessandria 15121 Alessandria, Italy
[3]STAR Integrated Research Unit, Università di Foggia, 71121 Foggia, Italy
[4]Istituto per lo Studio delle Macromolecole (ISMAC-CNR), 20133 Milano, Italy
[5]Dipartimento di Scienza e Tecnologia del Farmaco, Università di Torino, 10125 Torino, Italy
[6]Dipartimento di Scienze Agrarie, Università di Torino, Forestali e Alimentari, 10095 Grugliasco (TO), Italy
[7]National Polytechnic Institute of Toulouse, INP-ENSIACET Laboratory of Agro-Industrial Chemistry, 31030 Toulouse, France
Correspondence to: E. Montoneri (E-mail: enzo.montoneri@gmail.com)

ABSTRACT: Blended films were obtained from polyvinyl alcohol-*co*-ethylene (EVOH) with 52 kDa weight average molecular weight (M_w) and three water soluble biopolymers isolated from exhausted tomato plants hydrolysates. Two biopolymers contained mainly polysaccharides and had 27 and 79 kDa M_w, respectively. The third contained mainly lignin-like C moieties and had 392 kDa M_W. The films were fabricated with a biopolymer/EVOH w/w ratio ranging from 0.1 to 0.9. All blends had molecular weight and solubility which were substantially different from the starting materials. They were characterized for the chemical nature, and the thermal, rheological, and mechanical properties. Evidence of a chemical reaction between the biopolymers and EVOH was found. Generally, the films exhibited higher mechanical strength but lower strain at break then the neat EVOH. The best performing blended film was fabricated from the 27 kDa M_w polysaccharide. This contained less than 10% biopolymer. It exhibited 1043 MPa Young's modulus and 70% strain at break against 351 MPa modulus and 86% strain for neat EVOH. The results offer scope for investigating biopolymers sourced from other biowastes to understand more the reasons of the observed effects and exploit their full potential to modify or to replace synthetic polymers. © 2015 Wiley Periodicals, Inc. J. Appl. Polym. Sci. **2015**, *132*, 41935.

KEYWORDS: biomaterials; biopolymers & renewable polymers; blends; composites; films

Received 28 October 2014; accepted 2 January 2015
DOI: 10.1002/app.41935

INTRODUCTION

This work addresses two current important issues: (i) the valorization of agriculture residues as source of chemicals and (ii) the manufacture of biocompatible polymer blends. Agriculture residues contain natural polymers, such as cellulose, hemicelluloses, and lignin. Aside cellulose finding widespread use in the manufacture of articles for everyday life use, hemicelluloses and lignin are not suitable at the same purpose because of low molecular weight and lack of adequate mechanical properties. Synthetic polymers from fossil sources have a range of mechanical properties which allow manufacturing most of the articles currently used. However, due to their low biodegradability, they are not compatible with the environment. For this reason, current research trend pursuits the manufacture of biopolymers and/or of their blends with synthetic polymers.

Blends of synthetic polymers and biopolymers of agricultural sources are well known. Several blends of polyvinyl alcohol and vinyl alcohol-ethylene copolymers (EVOH) and polysaccharides such as starch[1] or lignocellulosic materials including corn fiber[2] and sugar cane bagasse[3] have been reported. These products have been proposed for manufacturing mulch films for use in agriculture. In these films, the synthetic polymer provides the required mechanical properties and is compatible with the lignocellulosic fillers by virtue of its hydroxyl and carboxyl groups. So far, postharvest tomato plants (PHTP) as source of lignocellulosic substances (LS) to blend with synthetic polymers

Additional Supporting Information may be found in the online version of this article.

Table I. List, Nomenclature, and Short Description of Materials Prepared in this Work

Nomenclature	Description
PHTP	Postharvest tomato plant
F*i*,*i* = 1–5	Soluble products obtained from PHTP according to Scheme 1.
IR*i*. *i* = 1–5	Insoluble products obtained from PHTP according to Scheme 1.
EVOH	Poly(vinyl alcohol-*co*-ethylene)
EVOH-F2 *R*, *R* = 0.1–0.9	Blend obtained from EVOH and F2 at F2/EVOH w/w ratio (*R*) 0.1–0.9
EVOH-F4 *R*, *R* = 0.1–0.2	Blend obtained from EVOH and F4 at F4/EVOH w/w ratio (*R*) 0.1–0.2
EVOH-F5 *R*, *R* = 0.1–0.5	Blend obtained from EVOH and F5 at F5/EVOH w/w ratio (*R*) 0.1–0.5

have not been investigated. Yet, the manufacture of mulch films using PHTP LS would be a rather desirable integration of chemistry with agriculture and the environment.

In this work PHTP sourced from the province of Ragusa, in south east Sicily, Italy, were hydrolyzed to separate the lignin and cellulose components, and the hydrolysates were used to manufacture several blends with EVOH. The rationale for investigating these specific materials stems from several reasons. First, worldwide tomato production[4] is estimated 150 million ton per year. Thus, abundance of postharvest residues from this culture is available. For viable exploitation, the material geographical concentration is, however, more important than the total amount. For the present work, PHTP were sourced from a location where cultivation is practiced intensively by 4168 farms in open field and green house installations distributed over 9156 ha area. These farms are located within 30 km of the centre of this area. They produce 25,000 ton per year postharvest horticulture residual dry matter, containing 20,000 ton organic matter.[5] The cultivation residues are currently burned at each farm site in the open field. Thus, a large amount of agriculture residues concentrated over relatively small area is produced in this part of Italy and needs more eco-friendly disposal practices. These geographic and production features guarantee the availability of a concentrated potentially cost-effective lignocellulosic waste feedstock. They make the above chosen location and its horticulture residues rather appealing for the installation of a biorefinery which was not critically burdened with feed material collection and transportation costs.

Secondly, previous work has shown that these specific agriculture residues are a rich source of LS,[6] which are also effective as plant biostimulants to use in further cultivation practices.[7] Thus the manufacture of EVOH blends containing these substances would benefit from the mechanical properties contributed by the synthetic polymer and from the hydrophilic functional groups and eco-compatibility of the LS. In addition, the blends fabricated with these LS would be ideal for the manufacture of mulch film to use in agriculture, where at the end of their service life might be exploited for their plant biostimulant properties.

Fourth, compared with dedicated crops, PHTP are a negative cost[8] residual material. Thus, partial substitution of EVOH with PHTP LS would imply a significant reduction of the cost impact of the starting components in the finished film product.

The present work reports the manufacture of EVOH-PHTP LS blends in film form, the chemical composition, the molecular weight, and the thermal and mechanical properties as a function of the LS nature and content.

EXPERIMENTAL

Materials

The materials and the nomenclature used in this work are listed and shortly described in Table I.

Postharvest Tomato Plants and Hydrolysates

Postharvest tomato plants were supplied by the Zocco farm in Rosolini (SR), Italy. This material (PHTP) was ground to less than 1 mm size by means of the SF75 mill by Cimma Spa, Pavia, Italy. The powder was then hydrolyzed at acid and/or alkaline pH to yield three products: i.e. F2, F4, and F5. Product F2 was obtained by refluxing PHTP in 1*M* HCl for 4 h at 10 v/w liquid/solid ratio. The resulting suspension was filtered to separate the acid hydrolyzate from the insoluble residue. The filtrate was evaporated at 40°C under vacuum. The F2 solid residue was recovered in 50% yield relatively to the starting PHTP weight. Product F4 was obtained by hydrolyzing PHTP in a pilot plant comprising an electrically heated mechanically stirred 500 L reactor, a 102 cm long × 10.1 cm diameter polysulfone ultra filtration membrane with 5 kDa molar mass cut-off supplied by Idea Engineering s.r.l. from Lessona (Bi), Italy, and a forced ventilation drying oven. According to the operating experimental conditions, PHTP was reacted 4 h with pH 13 aqueous KOH at 60°C and 4 v/w liquid/solid ratio. The liquid/solid mix was allowed to settle to separate the supernatant liquid phase containing the soluble hydrolysate containing F4 from the insoluble residue. The recovered hydrolysate was circulated at 40 L/h flow rate through 5 kDa cut off polysulfone ultra filtration membrane operating with tangential flow at 7 bar inlet and 4.5 bar outlet pressure to yield a retentate with 5 to 10% dry matter content. The concentrated retentate was finally dried at 60°C to yield the solid F4 in 10 wt % yield, relatively to the starting PHTP. Product F5 was obtained by heating at 60°C in concentrated HCl for 2 h the insoluble residue separated from the above F4 hydrolyzate. The solid/liquid acid suspension was centrifuged to separate the acid solution containing F5 from the insoluble residue. The former was dried under vacuum in a rotary evaporator and then stored over KOH and P_2O_5 to constant weight. The yield of solid F5 was 45% relative to the

$$\text{PHTB + BZ/EtOH 1/1} \xrightarrow{\text{Soxlet Extractor}} \text{F1 + IR1} \quad (1)$$

$$\text{IR1 + HCl 1M} \xrightarrow{\text{Reflux}} \text{F2 + IR2} \quad (2)$$

$$\text{IR2 + HCl 12M} \xrightarrow{\text{4°C}} \text{F3 + IR3} \quad (3)$$

$$\text{PHTB + NaOH} \xrightarrow{\text{60°C pH 13}} \text{F4 + IR4} \quad (4)$$

$$\text{IR4 + HCl 1M} \xrightarrow{\text{60°C}} \text{F5 + IR6} \quad (5)$$

Scheme 1. Scheme 1Chemical treatment of PHTP and its major components (IR = insoluble residue; F = soluble fraction).

starting alkali insoluble residue. Pellets of EVOH (poly(vinyl alcohol-*co*-ethylene), ethylene 38 mol %), commercial name Soarnol, CAS number 26221-27-2, were supplied by Nippon Gohsei Europe GmbH (Düsseldorf). All other reagents and solvents were supplied by Sigma Aldrich and used as purchased.

Preparation of EVOH-LS Films

EVOH pellets (10 g) were dissolved in 100 mL dimethyl sulfoxide (DMSO) under stirring at 120°C. The LS samples were dissolved in water at 50 to 80 g L^{-1} concentration. The solutions were centrifuged before use to separate any insoluble residue. Then, the appropriate amount of LS solution was added drop wise to the hot EVOH solution to allow water distillation and to obtain a final homogenous solution containing the desired amounts of EVOH and LS. Several samples were obtained following the above general procedure by varying the initial LS amount. Heating of this solution was continued to complete removal of the residual water added with LS as measured by the collected volume of the distilled water. The solution was then heated under vacuum to evaporate DMSO. The solvent evaporation was continued to obtain a viscous flowing liquid which could be poured and spread on a hot casting plate by doctor blade moving along the stationary casting surface. The resulting viscous wet layer was heated 3 h at 70°C in an oven to yield a film coating the casting plate surface. The assembly was then immersed in a water bath for at least 1 h to allow film detachment from the plate surface. The recovered free standing film was washed repeatedly with water to remove the residual DMSO and unreacted LS. This operation was repeated until the final collected water washing was colourless. The recovered films were dried by a fan blowing 40°C air and then stored over P_2O_5 to constant weight. Films of 150 μm thickness were typically obtained. The films were obtained from DMSO solutions containing LS and EVOH in the 0.1 to 0.9 LS/EVOH weight ratio range. The films obtained from the solutions containing LS and EVOH in the 0.1 to 0.4 LS/EVOH weight ratio range looked homogeneous and transparent. The films obtained at higher LS/EVOH weight ratio were too dark to let light go through, and therefore did not look transparent. All films could be bent at 180° angle without breaking. Neat EVOH films were prepared by the same solvent casting procedure using the above EVOH solution in DMSO, without addition of LS.

Determination of the Net Organic Matter (LSorg) Contributed by LS in the EVOH-LS Films

The organic fraction contributed by LS in the film was calculated based on elemental N analytical concentration values, according to eq. (1).

$$\text{LS}_{\text{org}} = \frac{\%N_f \cdot \text{VS}}{N} \quad (1)$$

In this equation VS and N are the volatile solids (wt %) and elemental N (wt %) contents in the neat LS sample, while N_f is the elemental N (wt %) content in the EVOH-LS film. The VS and N contents in the neat LS samples and in the EVOH-LS films were determined, respectively, by calcination at 650°C and by microanalysis, according to previously reported procedures.[9]

Molar Mass Characterization of EVOH-LS Films

The molecular characterization of neat EVOH was performed by a multiangle laser light scattering (MALS) absolute detector online to a size exclusion chromatographic (SEC) system.[10,11] The molecular characterization of neat LS in powder form and EVOH-LS films was performed by a conventional SEC system because EVOH-LS blends are multicomponent systems with different specific refractive index increment per unit concentration increment (dn/dc). The relative calibration of the conventional SEC system was performed by using Pullulan.[12] This material is a linear homopolysaccharide of glucose described as a α-(1,6)-linked polymer of maltotriose subunits. It is available from Sigma Aldrich[13] as set of 10 different polysaccharides analytical standards for GPC with molecular weight (M_W) comprised between 0.320 and 800 kDa. The SEC chromatographic system consisted of an integrated GPCV 2000 system from Waters (Milford, MA) equipped with two online detectors: a MALS Dawn DSP-F photometer from Wyatt (Santa Barbara, CA) and a 2414 differential refractometer (DRI) from Waters used as concentration detector. In conventional SEC only the online DRI concentration detector is used. In detail the SEC chromatographic experimental conditions were the following: for neat EVOH 2 PLgel Mixed C columns from Polymer Laboratories, dimethylacetamide (DMAc) + 0.05*M* LiBr as mobile phase, 80°C temperature, 0.8 mL min^{-1} flow rate, 100 μL injection volume, about 2 mg mL^{-1} sample concentration; for neat LS and EVOH-LS blends 2 Polar Gel (M and L) columns from Polymer Laboratories, 90% DMSO + 10% H_2O as mobile phase, 80°C temperature, 0.6 mL min^{-1} flow rate, 100 μL injection volume, about 1.5 mg mL^{-1} sample concentration.

Other Measurements

Gas chromatography-mass spectrometry (GC-MS) analyses were carried out after prior derivatization. In a typical derivatization, 10 mg of the sample was solubilized in 1 mL of pyridine. Then, 300 μL of *N,O-bis*(trimethylsilyl) trifluoroacetamide) was added to the solution. The mixture was heated for 45 min at 60°C under magnetic stirring. GC-MS analyses were performed using a GC Agilent 6890 (Agilent Technologies) fitted with a mass detector Agilent Network 5973, using a 30 m long capillary column, i.d. 0.25 mm and film thickness 0.25 μm, and temperature program from 80°C (3 min) to 300°C at 5°C min^{-1}. Fourier transform-infrared (FT-IR) spectra of neat films or LS KBr pellets were recorded in transmission mode in a Perkin Elmer Spectrum BX spectrophotometer equipped with DTGS detector and working with 16 scans at 4 cm^{-1} of resolution in the 4000 to 400 cm^{-1} range. Differential scanning calorimetry (DSC) was carried out using a Mettler-Toledo DSC 821e apparatus. Samples of about 5 mg were employed. The instrument was calibrated with high purity standards at 10°C min^{-1}. Dry nitrogen was used as purge gas. The following temperature

Table II. Concentration Values as mol % of Total C for Functional Groups and C Types[a] in PHTP and Scheme 1 Fractions[b]

Fraction	Al	NR and OMe	OR	OCO	Ph	PhOX	COY	C=O	(Ph + PhOX)/ OCO
PHTP	14.34	7.22	49.60	11.62	6.82	3.44	6.28	0.61	0.88
F2	25.61	9.25	47.43	3.09	0.00	0.00	14.61	0.00	0.00
F3	13.98	8.23	47.29	10.80	9.25	5.36	4.11	0.98	1.35
IR3	20.69	8.20	45.68	9.44	4.75	2.79	7.21	1.25	0.80
F4	47.38	9.39	10.39	2.19	11.50	3.81	14.37	0.97	6.99
IR4	5.00	7.97	58.98	13.19	7.00	3.66	2.97	1.22	0.81

[a] Aliphatic (Al), amine and methoxy (NR and OMe), alkoxy (OR), anomeric (OCO), aromatic (Ph), phenoxy and/or phenol (PhOX), carboxyl (COY), keto (C=O) C, R = alkyl C and/or H, X = alkyl and/or aryl C, and/or H, Y = amide N and/or OH.
[b] See Scheme 1.

program was used: heating at 20°C min^{-1} from 25 to 200°C, then cooling at −10°C min^{-1} to 25°C and finally heating again at 10°C min^{-1} to 200°C. Rheological tests were performed using an ARES strain controlled rheometer (Rheometric Scientific). The frequency sweep tests were performed at strain of 5.0% over a frequency range from 100 to 0.1 rad s^{-1} at 200°C using a parallel plate geometry ($d = 25$ mm). The cryo-milled film was placed between the preheated plates at 200°C and was allowed to equilibrate for approximately 5 min before each frequency sweep run. The distance between the plates was settled at 1 mm and a compressive constant force of 1.0 N was applied to the samples during the measurements.[14] The mechanical tests were performed using a dynamical-mechanical analyzer DMTA V (Rheometric Scientific). All tests were carried out at a temperature of 25°C using the rectangular tension geometry on specimen machined into bars with size of 20 × 5 × 0.15 mm with a gauge length of 10 mm. The stress–strain mechanical analysis was performed at a strain rate of 0.01 s^{-1} with a preload force of 0.01 N. Five measurements were carried out on different specimens for each sample.[15]

RESULTS AND DISCUSSION

Chemical Nature of Raw PHTP and PHTP LS

The chemical composition of PHTP was first analyzed for its proximate composition as reported in previous work.[6,7] This procedure, designed for biomass analytical purposes, is expected to separate the major biomass proximates on the basis of the components' solubility in benzene and in HCl at different temperatures (Scheme 1, steps 1–3). Formally, the different fractions isolated in steps 1 to 3 are expected to represent lipids and apolar compounds (F1), hemicellulose and proteins (F2), cellulose (F3), and lignin (IR3). In the case of PHTP these fractions were obtained in the following w/w % yields: 11.9 F1, 44.0 F2, 15.5 F3, and 28.4 IR3. Scheme 1 includes also two other treatments (steps 4 and 5) which were used in this work to improve the separation of the saccharides from lignin.

The raw PHTP and, the F and IR fractions recovered after solvent evaporation and/or drying were also analyzed by solid-state ^{13}C-NMR spectroscopy (see Supporting Information Figures S1 and S2). The ^{13}C spectra allowed to identify the C types and functional groups contributed by the major proximates: i.e. the alkoxy (OR) and anomeric (OCO) C contributed by saccharides moieties as in F2 and F3, the aromatic phenyl (Ph) and penoxy (PhOH) C contributed by lignin (IR3), and the other C atoms which are likely distributed over the four F1-F3 and IR3 fractions. The data are reported in Table II. It may be observed that for PHTP the sum of OR and OCO C is about 61% C, the OR/OCO ratio is about 4, and the sum of the aromatic (Ph and PhOH) and aliphatic C is about 25%. These figures are consistent with the fractions' yields obtained according to Scheme 1, steps 1 to 3: i.e. the sum of the F2 and F3 fractions totalling about 60%, the presence of 5 C atoms saccharides moieties indicating excess of hemicelluloses over cellulose moieties, and the 28.4% amount of the lignin IR3 fraction. The ^{13}C data for the isolated F2, F3, and IR3 fractions, however, show that the PHTP treatment according to Scheme 1 does not allow a definite separation between saccharides, protein, and lignin structures. Indeed, neither F2 nor F3 can be identified as pure hemicelluloses and cellulose, while the lignin IR3 fraction still contains 55% OR and OCO C. This is consistent with the fact that in nature polysaccharides, protein and lignin are not present as simple physical mixtures composing vegetable matter, but are bonded to each other in complex structures[9] resisting chemical treatment.

As the anomeric and the aromatic C atoms are respectively the main indexes of the presence of saccharide and lignin molecules, Table II reports also the (Ph + PhOX)/OCO ratio to measure the treatment efficiency to separate lignin from saccharide matter. The data show that the highest efficiency is obtained by hydrolyzing PHTP in KOH at 60°C and pH 13 (Scheme1, step 4).

This reaction yielded two products: i.e. F4 recovered in 10% yield upon drying the soluble hydrolyzate and IR4 as the alkali insoluble residue. It may be readily observed from Table II that, compared with all other fractions, F4 has the highest aromatic/anomeric C ratio, while IR4 has 9× lower aromatic/anomeric C ratio than F4. The IR4 residue was further hydrolysed in 1*M* HCl at 60°C. The liquid hydrolysate phase was separated from the insoluble residue (IR6) and dried to yield the F5 fraction.

The F2 and F5 fractions, recovered from the acid hydrolysates of PHTP and IR4, respectively, were analyzed for their elemental C and N, and volatile solids content. Table III shows that they were found to contain 44 and 55% inorganic matter, respectively. The fractions organic matter was analyzed by ^{1}H NMR and GC-MS spectroscopy.

Table III. Data[a] for Neat LS and EVOH, and for EVOH-LS Films Calculated According to eq. (1)

Sample	*N* (wt %)	VS (wt %)	LS_{org} (wt %)
F2	1.59	56.51	-
F4	5.03	72.70	-
F5	0.54	45.80	-
EVOH	0.0	99.2	
EVOH-F2 0.1[b]	0.08	99.7	2.84
EVOH-F2 0.2[b]	0.23	100	8.17
EVOH-F2 0.3[b]	0.33	100	11.73
EVOH-F2 0.4[b]	0.55	99.4	19.55
EVOH-F2 0.5[b]	0.51	98.5	18.13
EVOH-F2 0.6[b]	0.57	98.9	20.26
EVOH-F2 0.7[b]	0.58	98.5	20.61
EVOH-F2 0.8[b]	0.58	99.2	20.61
EVOH-F2 0.9[b]	0.52	97.4	18.48
EVOH-F4 0.1[b]	0.82	94.4	11.85
EVOH-F4 0.2[b]	0.75	96.7	10.84
EVOH-F5 0.1[b]	0.05	99.1	4.24
EVOH-F5 0.2[b]	0.16	99.7	13.57
EVOH-F5 0.3[b]	0.24	98.6	20.35
EVOH-F5 0.5[b]	0.26	98.7	22.05

[a] Concentration referred to dry matter.
[b] LS/EVOH weight ratio of raw materials in DMSO before film casting.

The ^{1}H spectra (shown in the Supporting Information) contained major signals at 3 to 4 ppm, typical of CH—X, X = OR, NH_2 protons in saccharide and/or amino acid moieties, at 5.3 ppm arising from the anomeric proton in saccharides, and smaller signals at 1 to 2.0 ppm assigned to protons in aliphatic C chains substituted by acetyl, amino, and/or amide functional groups.[16] Signals of protons bonded to unsaturated C, falling above 7 ppm, were absent or present with low intensity. Analysis by GC-MS spectroscopy confirmed that the F2 and F5 organic matter contained mainly hexose and pentose saccharides. The GC signal areas of these saccharides relative to the total signals' area of the chromatogram amounted to 76 and 88% for the F2 and F5 samples, respectively. The two fractions were found different also for the composition of the remaining matter. The F2 organic matter contained about 10% amino acids such as leucine, aspartic acid, glutamine, and proline, and 14% carboxylic acids such as pentanoic, butandioic, and citric acid. The F5 organic matter contained 12% carboxylated compounds such as glucofuranuronic acid, hexadecanoic acid, galactofuranuronic acid, galacturonic acid, glucopyranuronic acid, D-glycero-L-manno-heptonic acid-γ-lactone. The different compositions of the F2 and F5 fractions was also confirmed by IR spectroscopy. Figure 1 shows that the spectra of F2 and F5 contain absorption bands due to the vibrations of carboxyl and/or hydroxyl functional groups: i.e. —C═O(OH) at 1700 to 1720 cm^{-1}, —OH and/or C—NH at 1628 to 1631 cm^{-1}, C—O at 1000 to 1100 cm^{-1}. They, however, differ for relative intensities. The —C═O(OH)/(—OH, NH) bands intensity ratio is higher in the F2 spectrum, consistently with the higher relative concentration of COOH contributed by the amino acids and carboxylic acids. By comparison, it may be observed that F4 exhibits two main bands at 1630 and 1540 cm^{-1}. The strong intensity of the latter band, coupled to the absence of the band at 1700 to 1720 cm^{-1}, is likely due to the presence of relatively higher concentration of amide functional groups. Table III indeed shows that F4 was found to contain over five times higher amount of elemental N than F2 and F5. Based on the analytical data, the F2, F4, and F5 fractions provided three water soluble products which were different in chemical composition for the lignin and saccharides' composition. These materials had weight average molecular weight (M_w) of 79 (F2), 392 (F4), and 27 (F5) kDa (Table IV). They were used to manufacture the EVOH-LS blends reported hereinafter, and thus to investigate thermal and mechanical properties as a function of the LS nature and content.

Chemical Composition of EVOH-LS Films

Determining the chemical composition of the EVOH-LS films was rather difficult for several reasons. As LS are soluble in water, while EVOH is insoluble in water, during the water washing of the cast films from the DMSO solution, release of some LS in water occurred. Thus, the LS concentration in the final film was expected lower than that calculated from the EVOH and LS relative weights present in the DMSO solution before

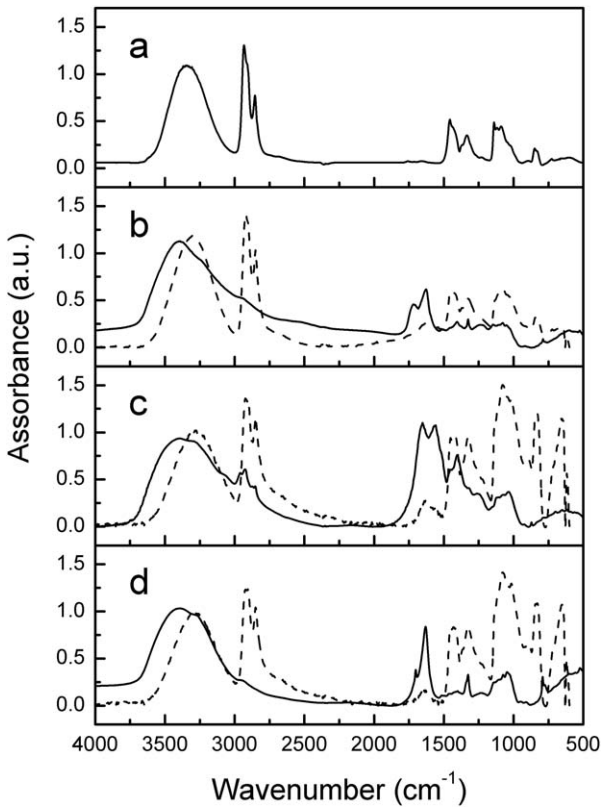

Figure 1. IR spectra of neat LS powder, and of neat EVOH and EVOH-LS films; solid line patterns for EVOH (a), F2 (b), F4 (c), and F5 (d); dotted line patterns for EVOH-F2 (b), EVOH-F4 (c), and EVOH-F5 (d) fabricated at 0.1 LS/EVOH w/w ratio.

Table IV. Macromolecular Features of Neat LS, Neat EVOH, and EVOH-LS Materials

Sample	M_p[a] (kDa)	M_w[b] (kDa)	M_w/M_n[c]	Mass recovery[d] (%)
EVOH	33.9	52.2	3.32	90.1
F2	16.8	79.0	3.14	100
F4	252.8	392.2	4.26	100
F5	14.3	27.4	1.46	100
EVOH-F2 0.1[e]	625.6	440.7	8.76	75.9
EVOH-F2 0.2[e]	471.3	265.9	5.57	36.7
EVOH-F2 1.0[e]	79.7	221.6	5.30	30.7
EVOH-F4 0.1[e]	170.2	165.4	2.96	100
EVOH-F4 0.2[e]	157.9	214.5	3.46	100
EVOH-F5 0.1[e]	35.6	154.7	4.46	83
EVOH-F5 0.2[e]	615.0	354.9	9.76	35.5
EVOH-F5 0.3[e]	579.9	384.3	7.72	26.1
EVOH-F5 0.4[e]	70.9	325.9	3.95	23.7
EVOH-F5 0.5[e]	124.9	299.9	2.21	10

[a] Molecular weight peak value.
[b] Weight average molecular weight.
[c] Polydispersity index.
[d] Sample mass recovery calculated from the chromatogram area.
[e] Raw materials weight ratio used in the films preparation.

casting the film. A second problem is that LS are mixtures of molecules containing the C types and functional groups listed in Table II. As these C moieties are likely not to be distributed homogeneously over the entire molecular pool constituting the neat materials, the molecules present in the film might have different chemical composition from those leached into the film

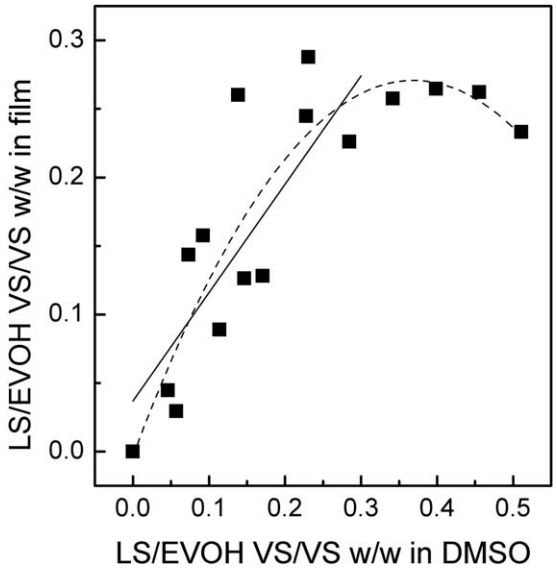

Figure 2. Plot of found LS/EVOH organic matter weight ratio in the film (LS/EVOH VS/VS w/w in film) against LS/EVOH organic matter weight ratio in DMSO before film casting; solid and dotted line fitted according to eqs. (2) and (3), respectively.

washing bath. A third problem is that the organic moieties listed in Table II comprise also aliphatic C atoms and OH functional groups which are hard to distinguish analytically from those belonging to EVOH. Under these circumstances N, present in LS and absent in EVOH, was investigated as candidate analytical probe element to assess the presence and possibly to calculate the concentration of LS in the films. Table III reports the raw analytical data obtained for neat EVOH, the neat LS components and the EVOH-LS films, and also the organic matter contributed by LS (LS_{org}) in the films calculated using eq. (1). In the table, the prepared film samples are identified by the type of LS and the LS/EVOH weight ratio referred to the raw materials present in the DMSO solution before casting the film.

Figure 2 reports the LS/EVOH VS/VS w/w ratio in the cast film against the LS/EVOH VS/VS w/w ratio in DMSO before film casting. Weight ratios are referred to the net organic matter. The film weight ratio is calculated from the experimental *N* and VS data in Table III. The DMSO weight ratio is calculated from the raw LS and EVOH VS data in Table III and the relative weights used in the preparation of the DMSO solution before casting the film.

The LS/EVOH ratio in the film (y) results directly proportional to the LS/EVOH ratio in DMSO (x) up to about 0.3 according to the eq. (2).

$$y = a + b \cdot x \tag{2}$$

The linear fit of the data in this range yields $a = 0.037 \pm 0.029$, $b = 0.79 \pm 0.16$, R^2 (correlation coefficient) = 0.82. Increasing the LS/EVOH ratio DMSO above 0.3 will not yield films with higher LS/EVOH ratio. The equation fitting the whole data pool is

$$y = a + b \cdot x + c \cdot x^2 \tag{3}$$

where $a = -0.003 \pm 0.030$, $b = 1.48 \pm 0.30$, $c = -2.01 \pm 0.57$, $R^2 = 0.87$.

Further support to the trend observed in Figure 2 was provided by IR spectroscopy. Figure 1 shows the *vis-a-vis* comparison of the IR spectra of the neat EVOH and LS materials and of the EVOH-LS films. It may be observed that the EVOH-LS are distinguished from the neat EVOH film by the presence of the bands falling in the 1500 to 1750 cm^{-1} wavelength range assigned to the vibrations of the carboxyl, hydroxyl, and amino functional groups of the molecules constituting the neat LS materials. These absorptions are mostly intense in the neat LS materials. Vice versa the absorptions at 2800 to 3000 cm^{-1} and below 1500 cm^{-1} are mostly intense in the neat EVOH sample. Figure 3 reports the plots of the absorbance ratio of the band at 1630 cm^{-1} to the band at 2850 cm^{-1} arising from the stretching vibration of aliphatic C—H bonds against the LS/EVOH weight ratios, both in the films and in DMSO. All plots yield linear regression coefficients comprised between 0.829 and 0.999. The data confirm the presence of LS materials in the blended films. The LS material remaining in the film has resisted the water washings of the films following their deposition. Thus the residual LS material in the film is no longer soluble in water as the pristine one. The change of solubility properties may suggest the occurrence of a chemical reaction

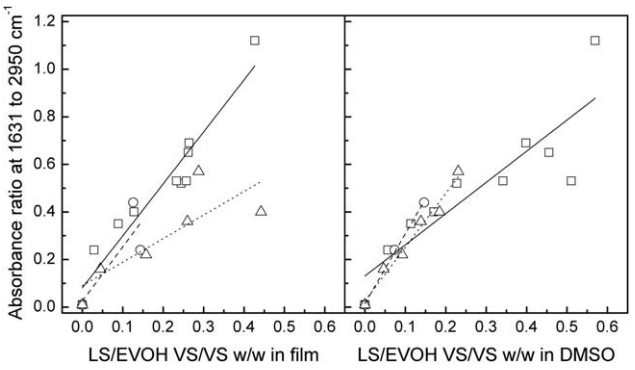

Figure 3. Plot of IR absorbance ratio versus LS/EVOH VS/VS w/w ratios in the film and in DMSO: EVOH-F2 (square symbol and solid line), EVOH-F4 (round circle and dashed line) and EVOH-F5 (triangle symbol and dotted line).

between LS and EVOH with formation of a new polymer containing EVOH macromolecules covalently bonded to LS molecules. The available samples cover a range of chemical compositions useful to investigate how the nature and concentration of LS affects the thermal and mechanical properties of the EVOH blends.

Macromolecular and Solubility Features of Neat LS and EVOH, and Blend EVOH-LS Films

The neat EVOH was completely soluble in DMSO, while the three neat LS samples were completely soluble in the mixed 90% DMSO + 10% H_2O solvent. Table IV reports the samples peak molecular weight (M_p), weight average molecular weight (M_w), and the polydispersity index M_w/M_n where M_n denotes the numeric average molecular weight. The data show that the three materials are polymeric. Given their source, they can be classified as biopolymers. The molecular weights features of neat F2 and F5 are comparable to those of neat EVOH. The M_w values of F2 and F5 are 79 and 24 kDa respectively, while the M_w value of EVOH is in between (52 kDa). These materials have also comparable polydispersity index, comprised between 1.5 and 3.3. The F4 samples has much higher M_w (392 kDa) and wider molecular weight distribution (MWD). Figure 4(A) shows the comparison of MWD of the three LS samples F2, F4, and F5. The higher M_w and wider MWD of F4 appear related to its higher lignin-like matter content. It appears from Figure 4 that F4 has two pools of macromolecules, one falling within the molecular weight range of the polysaccharide F2 and F5 materials (below 60 kDa), and the other in a much higher molecular weight range, above 100 kDa. Coupling this information with the chemical composition differences between these materials (see Chemical Nature of Raw PHTP and PHTP LS section), it seems quite likely that the F4 pool above 100 kDa consisted of lignin-like macromolecules, while the pool below 60 kDa contained mainly polysaccharide molecules. In between these two molecular pools, the third one comprised between 60 and 100 kDa might contain lignocellulosic molecules with mixed saccharide and lignin-like feature.

Very different it is the behavior in solution of the EVOH + LS blends (films). The blends between EVOH and LS generate strong interactions between the two components with a general increase of the apparent molecular weight and also a decrease of the sample solubility. Some blends in the 90% DMSO + 10% H_2O solvent are composed of soluble and insoluble fractions. Consequently, the molecular weight from SEC is related only to the soluble fraction. The molecular weight results of the three different series of EVOH-LS blends are reported in Table IV. The table also reports the sample mass recover, substantially the sample soluble fraction, calculated from the area of the chromatogram after an accurate calibration. It may be observed that for the F2 and F5 blends the mass recovery decreases from about 80% to 10% upon increasing the relative amount of the LS component in the blend. The soluble fractions of these blends show remarkably high M_w values comprised between 155 and 441 kDa. These values are far higher than those of the neat components comprised between 27 and 52 kDa. By comparison, the mass recovery for the two F4 blends is 100% and the M_w values are 165 to 214 kDa. In this case, the blend M_w value is comprised between that of neat EVOH (52 kDa) and that of neat F4 (392 kDa). In all cases, the increase of the EVOH-LS blends molecular weight compared with that of neat EVOH is remarkable, if one considers that this increase occurs already upon reacting EVOH with relatively small amounts of LS (i.e. 0.1 g of LS per g of EVOH for the EVOH-LS 0.1 blends). The blends molecular weight is rather higher than one could reasonably expect on the basis of the added amount of LS in the reaction mix and on a simple physical mixture of two separate components remaining distinct within a blend structure. Such molecular weight features could only be explained by imagining that the small amount of biopolymer molecules reacted to bridge several EVOH molecules. This reaction would lead to the increase of the molar mass of the F2 or F5 biopolymers, and of the synthetic polymer, in the EVOH-F2 and EVOH-F5 blends. The same occurs for the neat EVOH polymer present in large excess in the EVOH-F4 films. The solubility loss of the EVOH-F2 and EVOH-F5 blends is a further argument in favor of the chemical reaction occurring during the blend films preparation with formation of new high molecular weight polymers. As an example, the effect of the interaction between EVOH and the LS component is evident in Figure 4(B). The figure reports the comparison of the differential MWD for neat F2, neat EVOH, and the two EVOH-F2 blends. It clearly shows the increase of

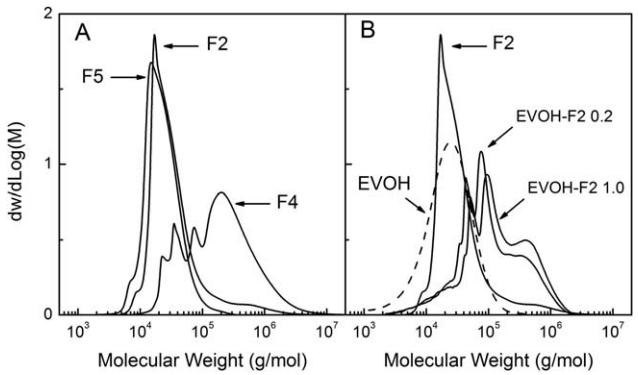

Figure 4. (a) Comparison of differential molecular weight distribution for F2, F4, and F5. (b) Comparison of differential MWD of neat F2, neat EVOH, EVOH-F2 0.2, and EVOH-F2 1.0 blends.

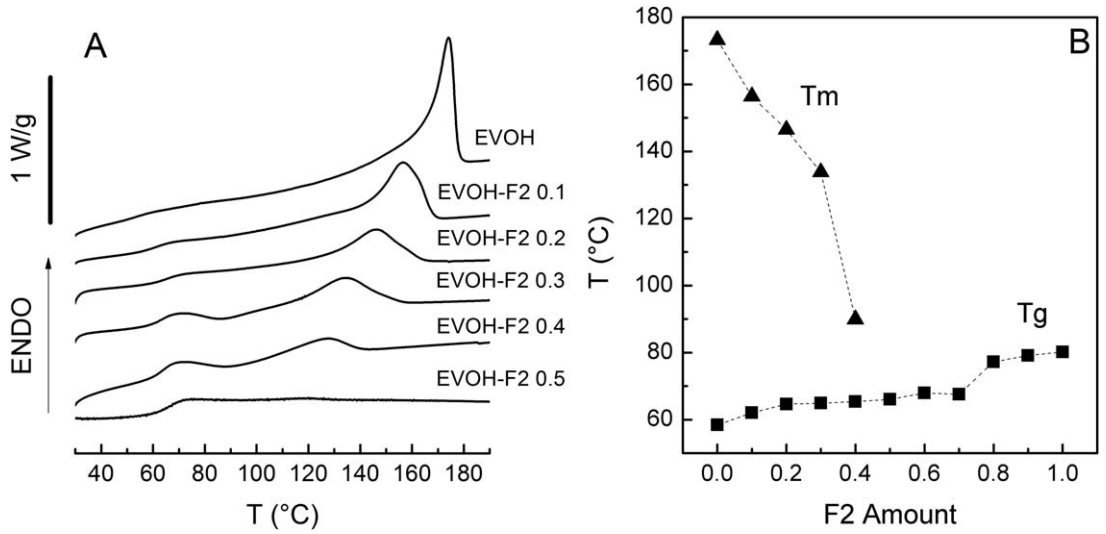

Figure 5. (a) DSC second heating at 10°C/min for EVOH-F2 blends and EVOH. (b) Trend of glass transition temperature T_g (■) and melting temperature T_m (▲) for sample series EVOH-F2 as a function of the F2 amount per unit EVOH used in the films preparation.

the molecular weight of EVOH-F2 with respect to neat F2. The behavior of EVOH-F4 and EVOH-F5 is consistent with the data in Table IV.

Films Thermal and Mechanical Behavior

As a typical example, Figure 5(A) reports the DSC second heating at 10°C/min for EVOH-F2 sample series, whereas the thermal data from the DSC measurements for sample series EVOH-F2, EVOH-F4, and EVOH-F5 are collectively reported in Table V. The thermal characteristics of the EVOH sample are in agreement with those previously reported by other authors.[17] The glass transition temperature (T_g) is not substantially affected by the presence of F4 and F5 in the films. It varies randomly from 53 to 61°C, showing no clear trend upon increasing LS

Table V. Thermal and Mechanical Data

Sample	T_g[a] (°C)	T_m[b] (°C)	ΔH_m[c] (J g^{-1})	Young's modulus (MPa)	Stress at yield point or maximum stress (MPa)	Strain at break (%)	Stress at break (MPa)
EVOH	58.2	173.8	58.0	352 ± 10	33 ± 2	86 ± 2	26 ± 1
EVOH-F2 0.1[d]	62.0	156.3	39.1	747 ± 36	43 ± 3	35 ± 2	32 ± 2
EVOH-F2 0.2[d]	64.6	146.5	25.6	689 ± 26	60 ± 4	12 ± 3	60 ± 4
EVOH-F2 0.3[d]	64.5	133.8	23.5	434 ± 31	55 ± 2	25 ± 7	55 ± 2
EVOH-F2 0.4[d]	64.9	126.5	5.3	505 ± 12	35 ± 4	15 ± 4	35 ± 4
EVOH-F2 0.5[d]	65.6	-	-	618 ± 10	65 ± 3	16 ± 6	65 ± 3
EVOH-F2 0.6[d]	68.0	-	-	725 ± 20	36 ± 2	10 ± 2	36 ± 2
EVOH-F2 0.7[d]	67.6	-	-	568 ± 14	53 ± 2	42 ± 4	53 ± 2
EVOH-F2 0.8[d]	77.2	-	-	559 ± 19	44 ± 2	17 ± 2	44 ± 2
EVOH-F2 0.9[d]	79.1	-	-	770 ± 35	64 ± 3	17 ± 2	64 ± 3
EVOH-F2 1.0[d]	80.2	-	-	480 ± 40	50 ± 3	8 ± 2	50 ± 3
EVOH-F4 0.1[d]	58.8	174.2	48.2	389 ± 15	44 ± 2	14 ± 3	41 ± 2
EVOH-F4 0.2[d]	61.3	175.8	47.5	381 ± 12	23 ± 2	12 ± 2	23 ± 2
EVOH-F5 0.1[d]	53.9	165.6	40.0	1043 ± 100	39 ± 3	70 ± 10	32 ± 1
EVOH-F5 0.2[d]	58.5	173.7	46.8	547 ± 23	22 ± 3	15 ± 4	22 ± 3
EVOH-F5 0.3[d]	54.6	173.1	48.3	188 ± 15	10 ± 1	10 ± 2	10 ± 1
EVOH-F5 0.4[d]	56.9	172.8	48.3	-	-	-	-
EVOH-F5 0.5[d]	52.6	174.0	31.8	-	-	-	-

[a] Glass transition temperature estimated at the midpoint.
[b] Melting temperature.
[c] Melting enthalpy.
[d] Raw materials weight ratio used in the films preparation.

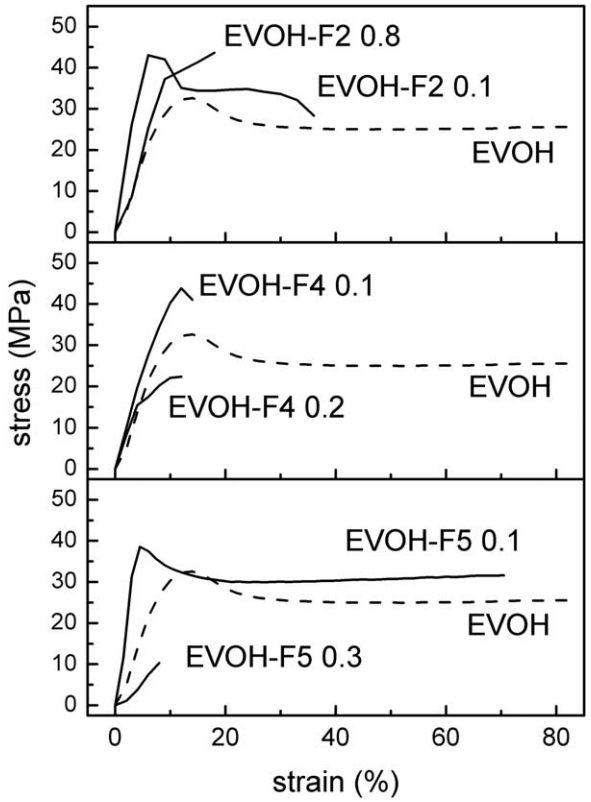

Figure 6. Stress–strain curves for EVOH-LS films.

concentration in the films. On the contrary, the EVOH-F2 samples exhibit increasing T_g from 58 to over 80°C upon increasing the F2 relative amount in the films [Figure 5(B)]. A similar trend occurs for the melting temperature (T_m). In sample series EVOH-F4 and EVOH-F5, the melting temperature varies from 173 to 176°C, with the only exception of EVOH-F5 0.1 sample for which the melting occurs at 166°C. For EVOH-F2, T_m decreases from 173 to 127°C upon increasing F2 up to 0.4 weight ratio [Figure 5(B)]. The presence of LS decreases the melting enthalpy of the EVOH in the various films. This decrease appears particularly pronounced in case of EVOH-F2 films which result completely amorphous at LS/EVOH weight ratio above 0.4.

The decrease of crystallinity suggests a high dispersion degree, possibly promoted by the occurrence of the chemical reactions between EVOH and LS.

All films had mechanical consistency which allowed their handling and bending at 180° angle without breaking. The various samples were subjected to a stress–strain analysis at 0.01 s^{-1} strain rate in order to investigate the effect of the LS addition on the modulus and its ultimate mechanical properties. Figure 6 reports the stress–strain curves for some EVOH-LS films. The mechanical data of all the samples are summarized in Table V. The strain at break and Young's modulus of neat EVOH film are 86% and 352 MPa, respectively, according to the literature.[17] As observed for the thermal properties, F2 blends resulted in a significant change of mechanical properties. This trend has been reported also for other blends containing polyvinyl alcohol (PVA) such as PVA/algae,[18] PVA/corn fiber,[2] PVA/hyaluronic acid,[19,20] PVA/sugar cane bagasse.[3] In essence, upon increasing F2 concentration in the film, the Young's modulus increases to an average 610 MPa value and the strain at break decreases from 86% in neat EVOH to 35 to 10% across the 10 samples fabricated at 0.1 to 1.0 F2/EVOH weight ratio. Similarly, the EVOH-F4 0.1 sample exhibits Young's modulus and stress at the yield point higher than neat EVOH, but very low strain at break. The best mechanical properties are exhibited by EVOH-F5 0.1 sample. Compared with neat EVOH and all other samples, this sample has the highest Young's modulus and stress at the yield point, but this is the only sample which maintains a relatively high strain at break.

The EVOH-F5 0.1 film was further investigated for its viscoelastic behavior in comparison with neat EVOH. Figure 7 reports the G', G'', and tan δ trends as a function of the frequency for this film. The viscoelastic behavior is different from neat EVOH. At low frequency, neat EVOH seems to obey the linear viscoelasticity model predictions[21,22] according to which the storage modulus G' results proportional to square of the frequency (ω^2) and loss modulus G' to the frequency ω. At low frequency, for the EVOH-F5 0.1 sample, the storage modulus G' exhibits a "pseudo solid-like behavior." This behavior is similar to the one previously described[23] and suggests the occurrence of a chemical reaction between EVOH and LS with formation of a branched polymer containing F5 covalently bonded to EVOH. This polymer is likely to be amorphous. According to the ΔH_m

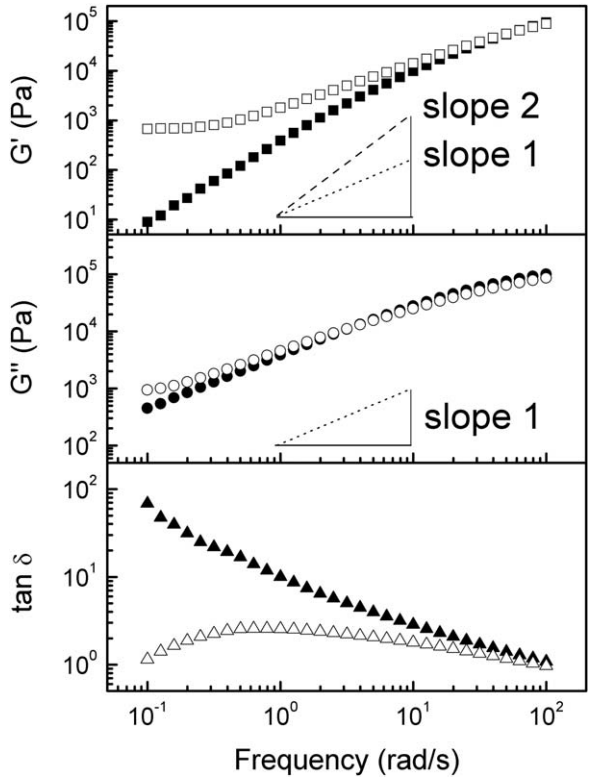

Figure 7. Trends of G', G'', and tan δ as a function of frequency for neat EVOH (full symbols) and EVOH-F5 0.1 (open symbols) at 200°C. Figure inserts indicate log G' vs. log ω plots in the low frequency region with slope values of 1 (slope 1) and 2 (slope 2).

values in Table V, the new branched amorphous polymer coexists together with the pristine crystalline EVOH.

All together the results of this work point out that the reaction of EVOH and LS during the film fabrication affects greatly the molecular weight and the properties of the pristine materials, very likely due to the formation of new higher molecular weight EVOH bonded to the biopolymer. In the new product, the pristine biopolymer molecules are no longer soluble in water and EVOH loses its crystallinity. The film containing less than 10% LS exhibit higher Young's modulus and stress at yield point than neat EVOH. Strain at break, however, is poor except for the film fabricated from EVOH and F5 at 0.1 F5/EVOH weight ratio. This film exhibits 70% strain at break compared with 86% for neat EVOH. Films containing higher concentration of LS have very poor mechanical properties. The available data do not allow understanding the reason of the peculiar behavior of F5 compared with the other LS materials. We can only observe that, compared with all other EVOH-LS blends in Tables III and IV, this material has the lowest molecular weight (165 kDa), keeps a good 64% crystallinity and exhibits a good 83% solubility in 90% DMSO–10% H_2O.

Cost, Environmental Implications, and Alternatives for Films Manufacture

A few questions need to be answered in order to evaluate the feasibility of developing to industrial commercial scale the herewith proposed material recycling technology for municipal biowaste to be utilized as composite films. These are (i) the residual DMSO solvent in the cast films, (ii) its environmental impact in the intended film application, (iii) the comparison of casting versus melting for the films fabrication, and (iv) the effects of the manufacture process on the film properties. To answer these questions, it should be considered first that DMSO is a common solvent in the chemical industry. It has a range of properties helping to meet process and product performance requirements. Basically, in addition to being a strong solvent for a variety of organic compounds including polymers, DMSO is completely miscible with water, safe to humans, and biodegradable in the environment, and recyclable using distillation technology.[24,25] These properties have been exploited in the laboratory manufacture of the EVOH-LS films, where the DMSO solvent was removed from the cast film by washing it with water and recovered by distillation. Technology at industrial level for film casting from organic solvents and solvent recovery, in compliance with safety regulations, is well developed.[26]

Solvent casting is ideal for manufacturing films containing heat sensitive substances because the temperature required for removing the solvent are usually lower than those for a hot-melt extrusion process. In the case of DMSO boiling at 189°C at atmospheric pressure, the solvent can be removed even at 50°C upon reducing the pressure to 6.6 mbar. Preliminary data (not included in this article) have indicated that EVOH-LS composites can be obtained by hot-melt extrusion at 200°C. This opens new technological perspectives. It offers worthwhile scope for research aiming to compare hot-melt extrusion versus solvent casting in relation to process cost and product performance. Future work along these directions will also allow to address another important issue: i.e. the composite films obtained are biodegradable or not? Data to answer this question have not been collected in the present work. Product biodegradability may be affected by the film fabrication technology. Thus, it will require a dedicated work once both the cast and the extruded films will be available.

CONCLUSIONS

New materials are obtained starting from a synthetic polymer with hydroxyl functional groups (EVOH) and biopolymers isolated from exhausted tomato plant hydrolysates containing saccharides and/or lignin matter. Evidence has been provided for a chemical reaction occurring between EVOH and the biopolymers yielding products in which the biopolymer is covalently bonded to the synthetic polymer. In this fashion, the biopolymer molecules modify the thermal, rheological, and mechanical properties of the pristine synthetic polymer. Similar effects are reported in literature for blends made from polyvinyl alcohol (PVA) and natural materials such as PVA/algae,[18] PVA/corn fiber,[2] PVA/hyaluronic acid,[19] PVA/sugar cane bagasse.[3] It has been found in the present work that the biopolymers increase the yield strength of the synthetic polymer if present at low concentration (less than 10%). The best mechanical performance was exhibited by the EVOH-F5 0.1 film. This film, compared with neat EVOH, exhibited higher Young's modulus and stress at yield point while maintaining a good 70% strain at break versus 86% for neat EVOH. The results offer scope for further process development work for these materials and biodegradability studies. It is also worthwhile to investigate biopolymers sourced from other biowastes to understand more the reasons of the observed effects and exploit their full potential to modify synthetic polymers. The valorization of agriculture residues as source of chemicals for the manufacture of biocompatible polymer blends is a realistic feasible goal from which economic and environmental benefits are expected for the chemical industry, agriculture and waste management practices.

ACKNOWLEDGMENTS

This work was funded by the Ministero delle Politiche Agricole e Forestali with the Agrienergia project. It was carried out also within the framework of the COST-European Cooperation in Science and Technology EUBis Action TD1203, specifically through the COST-STSM-TD1203-18837. The cooperation between the authors F. Franzoso, E. Montoneri, and C. Vaca Garcia was agreed at the workshop on Biorefinery for the Production of Energy and Biobased Products held in Torino on October 29 to 30, 2013 which was cofunded by the EUBis Action TD1203.

REFERENCES

1. Bastioli, C.; Bellotti, V.; Del Giudice, L.; Gilli, G. *J. Environ. Polym. Degrad.* **1993**, *1*, 181.
2. Cinelli, P.; Chiellini, E.; Lawton, J. W.; Imam, S. H. *J. Polym. Res.* **2005**, *13*, 107.
3. Chiellini, E.; Cinelli, P.; Solaro, R.; Laus, M. *J. Appl. Polym. Sci.* **2003**, *92*, 426.

4. UNCTAD. Organic fruit and vegetables from the tropics; **2003**. Available at: http://www.unctad.info/e.n/Infocomm/AACP-Product/COMMODITY-PROFILETomato. Accessed on 12 November 2014.
5. Personal communication from Prof. O. Sortino, also published in the following article available only in Italian. Sortino, O.; Sanzone, E.; Cartabellotta, D. Spec. Biomass. **2008**, *24*, 26.
6. Tabasso, S.; Montoneri, E.; Carnaroglio, D.; Caporaso, M.; Cravotto, G. *Green Chem.* **2014**, *16*, 73
7. Baglieri, A.; Cadili, V.; Mozzetti Monterumici, C.; Gennari, M.; Tabasso, S.; Montoneri, E.; Nardi, S.; Negre, M. *Sci. Horticult.* **2014**, *176*, 194.
8. Sheldon-Coulson, G. A. Production of Levulinic Acid in Urban Biorefineries; MA: Institue of Technology, **2011**.
9. Montoneri, E.; Boffa, V.; Savarino, P.; Perrone, D. G.; Montoneri, C.; Mendichi, R.; Acosta, E. J.; Kiran, S. *Biomacromolecules* **2010**, *11*, 3036.
10. Mendichi, R.; Giacometti Schieroni, A. *Curr. Trend Polym. Sci.* **2001**, *6*, 17.
11. Wyatt, P. *J. Anal. Chim. Acta* **1993**, *272*, 1.
12. Pullulan, T. D. Biopolymers online; **2005**. Available at: http://www-wiley.vch.de/books/biopoly/pdf_v06/bpol6001_1_11.pdf10. Accessed on 12 November 2014.
13. Sigma-Aldrich. Pullulan Standard Set; **2003**. Available at: http://www.sigmaaldrich.com/catalog/product/fluka/96351?lang=it&region=IT. Accessed on 12 November 2014.
14. Mauro, N.; Manfredi, A.; Ranucci, E.; Procacci, P.; Laus, M.; Antonioli, D.; Mantovani, C.; Magnaghi, V.; Ferruti, P. *Macromol. Biosci.* **2013**, *13*, 332.
15. Renò, F.; Carniato, F.; Rizzi, M.; Marchese, L.; Laus, M.; Antonioli, D. *J. Appl. Polym. Sci.* **2013**, *129*, 699.
16. Montoneri, E.; Savarino, P.; Adani, F.; Genevini, P. L.; Ricca, G.; Zanetti, F.; Paoletti, S. *Waste Manag.* **2003**, *23*, 523.
17. Nir, Y.; Narkis, M.; Siegmann, A. *Polym. Eng. Sci.* **1998**, *3*, 1890.
18. Chiellini, E.; Cinelli, P.; Ilieva, V. I.; Martera, M. *Biomacromolecules* **2008**, *9*, 1007.
19. Lazzeri, L.; Barbani, N.; Cascone, M. G.; Lupinacci, D.; Giusti, G.; Laus, M. *J. Mater. Sci. Mater. Med.* **1994**, *5*, 862.
20. Cascone, M. G.; Laus, M.; Ricci, D.; Sbarbati del Guerra, R. *J. Mater. Sci. Mater. Med.* **1995**, *6*, 71.
21. Ferry, J. D. Viscoelastic Properties of Polymers; Wiley: New York, **1980**.
22. Haley, J. C.; Lodge, T. P. *J. Rheol.* **2004**, *48*, 463.
23. Franzoso, F.; Tabasso, S.; Antonioli, D.; Montoneri, E.; Persico, P.; Laus, M.; Mendichi, R.; Negre, M. *J. Appl. Polym. Sci.* **2015**, *132*, 41359.
24. Gaylord Chemical Company. L.L.C. Bulletin 165B; **2008**. Available at: http://www.gaylordchemical.com/uploads/images/pdfs/literature/165B.pdf. Accessed on 12 November 2014.
25. Gaylord Chemical Company L.L.C. DMSO technical bulletin.pdf, Slidell, LA.
26. Siemann, U. *Progr. Colloid Polym. Sci.* **2005**, *130*, 1.